

Discontinuities in the Long-Term Northern Hemisphere 500-Millibar Heights Dataset

STEVEN J. LAMBERT

Canadian Climate Centre, Downsview, Ontario, Canada

16 January 1990 and 16 May 1990

ABSTRACT

Using time series of simple statistics, the homogeneity of a long-term Northern Hemisphere 500-mb dataset is assessed. Several discontinuities coinciding with major analysis changes were found which indicate that care must be exercised in the use of this dataset in studies where homogeneous data are required.

1. Introduction

Recent concern about climate change and the behavior of the atmosphere on long time scales has renewed interest in long-term datasets. For example, a long-term 700-mb dataset produced by the National Meteorological Center (NMC) containing data from about 1950 onwards has been used for a variety of studies, such as Esbensen (1982) who examined Northern Hemisphere teleconnection patterns and Barnston and Livezey (1987) who studied the low-frequency circulation using orthogonally rotated principal component analysis (RPCA). An even longer-term dataset is the Northern Hemisphere 500-mb geopotential heights dataset, available from the National Center for Atmospheric Research (NCAR). This dataset provides a more or less continuous record of daily values since 1 January 1946, and is particularly attractive because it is the longest running readily available upper-air dataset giving complete coverage of the extratropical Northern Hemisphere. It is also possible to use it to compute mean lower tropospheric temperatures based on the 500–1000 mb thickness field. Suitable 1000-mb heights can be obtained from long-term mean sea level pressure analyses such as those described in Trenberth and Paolino (1980).

If this dataset is to be used for climate change studies, then its reliability must be assessed in some manner to ensure that the effects of changing analysis techniques are not confused with the effects of changing climate. This is done in the present study by computing time series of simple statistics in order to search for discontinuities. Such discontinuities would indicate that the dataset must be used with caution and that the presence of the discontinuities must be taken into

account when interpreting the results of studies based on these data.

2. Data

The dataset was assembled by NCAR using data from a variety of sources as described in Jenne (1975). The data are available once per day beginning in 1946 on the standard 1977-point Northern Hemisphere polar stereographic grid used at the NMC. Since the historical data were archived in different formats, various transformations were applied to place the data on a common grid. From January 1946 to December 1952 the data were derived from manually digitized values produced by the US Navy Applied Research Operational Weather Analysis (AROWA) Project. Point values were extracted from hand analyses at the corners and the centers of $10^\circ \times 10^\circ$ latitude–longitude quadrangles forming a diamond grid with a grid spacing of about 7° (Berry et al. 1953). These point values were later objectively analyzed by the Fleet Numerical Weather Central (FNWC) to give values on the standard NMC grid. From January 1953 to March 1955 manually analyzed charts were digitized at the National Climatic Center (NCC) using a curve follower. The extracted values along the contour lines were then objectively analyzed to the NMC grid by FNWC. From April 1955 to March 1960 the data originated from the 433L Electronics Support System Project Office (433L ESSPO). For this period, values were read from the hand analyses of the National Weather Analysis Center (NWAC), a forerunner of the NMC, at every second point on the NMC grid [USAF Weather Observing and Forecasting System, 433L (1959)]. The remainder of the grid points were obtained by interpolation. From April 1960 to December 1961 the data are NMC analyses archived by the Air Force Global Weather Central (AFGWC). The data were sent to AFGWC by teletype and only every second point was transmitted. In January 1962 AFGWC's own objective

Corresponding author address: Steven J. Lambert, Numerical Modeling Division, Canadian Climate Centre/CCRN, 4905 Dufferin Street, City of North York, Downsview, Ontario, Canada M3H 5T4.

analysis scheme became operational and as a result from January 1962–November 1962 the dataset contains the AFGWC analyses which were done at the NMC grid points. From December 1962 onward the dataset contains NMC operational analyses which were archived at analysis time without further modification. The analysis procedures used at the NMC continually evolve as improvements are incorporated and such changes could induce discontinuities. These changes will not be discussed unless there is an accompanying discontinuity in the statistics.

It is clear that changes in the character of the observing system that provides the raw data could also have an effect on the analyses. It is difficult to determine the radiosonde station distribution for the entire period since 1946, and even if one did know the station distribution it would not be clear which stations were used in the analyses and which were rejected. Oort (1983) gives the geographical distribution of radiosonde stations reporting 500-mb data at 6-month intervals from July 1958–January 1973. In July 1958 there were approximately 260 stations north of 30°N. These stations were not uniformly distributed, leaving data sparse areas in the Pacific, Atlantic, and Arctic Oceans. From 1958 to 1973 the number of radiosonde stations increased slowly reaching about 500 by 1973. Even though there was a twofold increase in the total number of stations, the number in the Pacific and Atlantic remained essentially constant. Since the configuration of the observing system changed slowly in time, it is unlikely that changes would result in discontinuities but rather they would result in artificial trends.

There was a worldwide change in the observing system that took place on 1 June 1957. On this date the release times of the radiosondes were changed from 0300 UTC to 0000 UTC and from 1500 UTC to 1200 UTC. It is likely that weak discontinuities were introduced with this change.

3. Analysis

The search for discontinuities introduced by the analysis changes is done by computing monthly anomalies of various quantities from 30°N to the North Pole for the period January 1946–December 1989. The anomalies, X_{ym}^a , are obtained from the daily values, X_{ydm} , (where y is the year, $y = 1946, \dots, 1989$; m is the month, $m = 1, \dots, 12$; d is the day, $d = 1, \dots, d_m$; and d_m is the number of days in the month) by

$$\bar{X}_{ym}^a = \bar{X}_{ym\cdot} - \bar{X}_{\cdot m} \quad (1)$$

where the overbar represents an average over the indices replaced by dots and X denotes an average over all grid points north of 30°N. Anomalies are calculated for three quantities; the geopotential, Φ , the transient eddy variance of the geopotential, $\Phi'\Phi'$, (the prime represents a deviation from the monthly mean), and the kinetic energy (KE) of the geostrophic wind, K_g , computed from the heights using finite differences.

4. Results

The top panel of Fig. 1 shows the time series of the monthly geopotential anomaly from January 1946 to December 1989. The dashed vertical lines mark the times of the analysis changes. There are three discontinuities evident in the time series. The first occurs in 1955 coincident with the introduction of the ESSPO analyses, which resulted in a decrease of about $100 \text{ m}^2 \text{ s}^{-2}$ in the average geopotential. A second discontinuity of similar magnitude accompanies the transition to the NMC operational analyses in 1962. A weaker third discontinuity of $50 \text{ m}^2 \text{ s}^{-2}$ is present in late 1978 when the NMC began using an optimum interpolation analysis system. No obvious trends are visible in the time series and the approximate $150 \text{ m}^2 \text{ s}^{-2}$ change in the

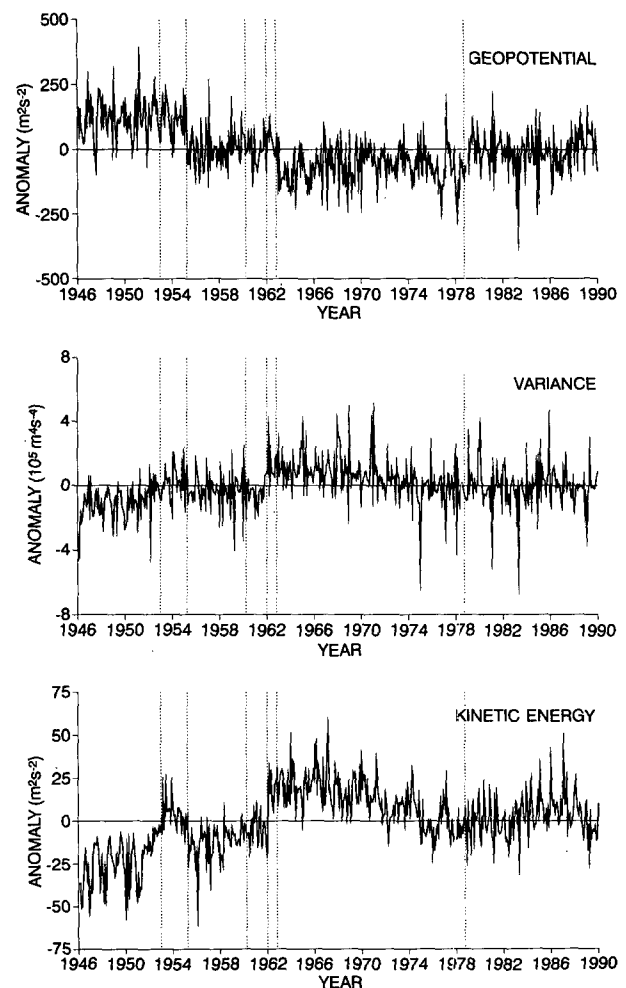


FIG. 1. Monthly geopotential anomalies in $\text{m}^2 \text{ s}^{-2}$ (top), monthly transient eddy variance anomalies in $10^5 \text{ m}^4 \text{ s}^{-4}$ (middle), and monthly geostrophic kinetic energy anomalies in $\text{m}^2 \text{ s}^{-2}$ (bottom) computed using data from the Northern Hemisphere 500-mb dataset between 30°N and the North Pole for the period January 1946–December 1989. The vertical dashed lines mark the times of major analysis changes described in the text.

mean geopotential between 1946–1989 is essentially the result of the discontinuities.

Barnston and Livezey (1987) detected discontinuities of similar magnitude in the subtropics in the mid-1950s in a study that used 700-mb analyses produced by the NWAC and the NMC. Given the high degree of correlation between 700-mb heights and 500-mb heights, it is likely that the discontinuities found by Barnston and Livezey and that found in the mid-1950s in the present study are related even though they occurred about a year and one-half apart. The Barnston and Livezey study did not detect discontinuities in the extratropics because their search technique was concerned with standardized anomalies, and the increased variability in the midlatitudes compared to the subtropics reduces the statistical significance of midlatitude discontinuities. The present study was able to detect a jump in the extratropics because of the large number of degrees of freedom that were combined when forming the hemispheric averages.

The time series of the $\Phi'\Phi'$ anomalies is shown on the middle panel of Fig. 1. Discontinuities coincident with the analysis changes are not so clear as those of the geopotential. The anomalies tend to be negative with a slight increasing trend from 1946 to 1952 when the data were from Project AROWA. During the period 1953–1955 when the hand analyzed charts were digitized using a curve follower, the anomalies tend to be slightly positive. There appears to be a discontinuity in April 1955 coincident with the incorporation of the ESSPO data and from April 1955 to 1961, the anomalies are generally negative with no noticeable trend. With the introduction of operational analyses in 1962,

the anomalies generally become positive and exhibit a decreasing trend from 1962 to 1989.

The K_g anomalies are shown on the bottom panel of Fig. 1. Since this quantity depends on the square of the horizontal gradient of the geopotential, it is sensitive to the horizontal resolution of the dataset. During the Project AROWA analysis period 1946–1952 when the hand analyses were digitized on a relatively coarse grid, the anomalies are negative with an increasing trend. There are suggestions of discontinuities flanking the period 1953–1955 when the curve follower was used to digitize the maps. The curve follower would be expected to preserve the detail present in the original hand analyses and thus would represent an increase in resolution over the preceding analyses. During this time the anomalies are generally positive. From 1955 to 1961 the anomalies again become negative as a relatively coarse grid, having $2^{0.5}$ times the grid spacing of the NMC standard grid, was used in the digitizing. With the introduction of the AFGWC operational analysis on the NMC grid in 1962, there is a very sharp discontinuity in the time series. From 1962 onward there is a general decreasing nonlinear trend in the K_g anomalies.

For all of the discontinuities, the mean of the 24 months preceding the discontinuity was tested against the mean of the 24 months following the discontinuity using a t -test. In all cases, the discontinuity was significant at the five percent level. Although this test is not definitive, it does support the occurrence of the discontinuities.

The preceding results indicate that there are indeed discontinuities in the 500-mb dataset and that they coincide with major analysis changes. With the exception of the change from the ESSPO analyses to the AFGWC analyses in April 1960, all the analysis changes described previously are accompanied by discontinuities. The year 1962 is particularly inhomogeneous since two analysis changes were introduced during that year.

The anomalies for the winter season (Dec–Feb) and the summer season (Jun–Aug) were examined separately to ascertain the seasonal dependence of the results. The discontinuities in the geopotential were present in both seasons with equal magnitude. For the variance and the KE, the discontinuities were larger by a factor of two in the winter season. In all cases, the discontinuities in summer were visually more apparent than in winter as a result of the reduced scatter of the anomalies in summer.

The area north of 30°N was divided into six subregions (see Fig. 2) in order to determine if the hemispheric discontinuities were the result of localized discontinuities caused, for example, by problems in data sparse areas or were the jumps truly hemispheric in scope. The regional anomalies were computed from (1) by averaging over all grid points contained in each region. The reduced area of each subregion resulted in increased scatter of the monthly anomalies, which ne-

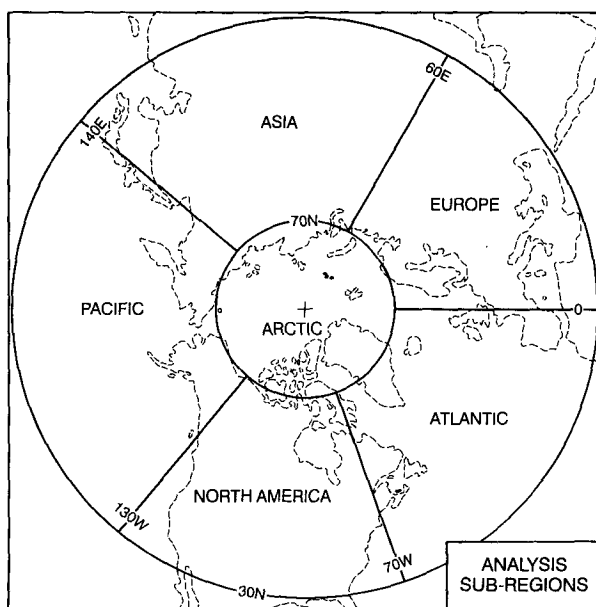


FIG. 2. The subregions used in the regional analysis.

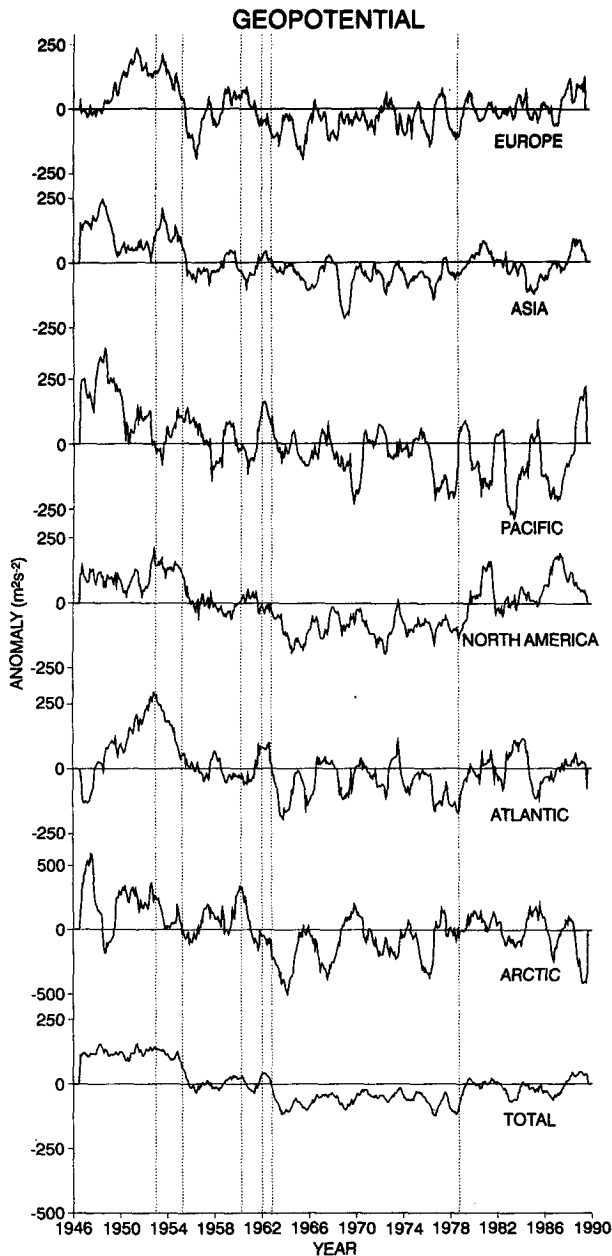


FIG. 3. Time series of the monthly geopotential anomalies in units of $\text{m}^2 \text{s}^{-2}$ averaged over each of the subregions and the total area north of 30°N . The time series have been smoothed using a 12-month running-mean filter. Note the change of scale for the Arctic results.

cessitated the application of a 12-month running mean filter to smooth the results.

The filtered time series of Φ for the six subregions as well as for the total area north of 30°N are displayed in Fig. 3. Clearly, there is an unequal contribution to the anomalies from each of the subregions. The 1955 discontinuity is evident only in the relatively well-ob-

served land subregions of Europe, Asia, and North America with little indication of discontinuities in the three oceanic subregions except for the Atlantic. The reason for this is not clear since one would expect analysis changes to be felt most in data sparse areas. The 1962 discontinuity arises principally from the Atlantic and the Arctic subregions, and the 1978 jump is most apparent in the North America subregion with lesser contributions from the Atlantic and Asia.

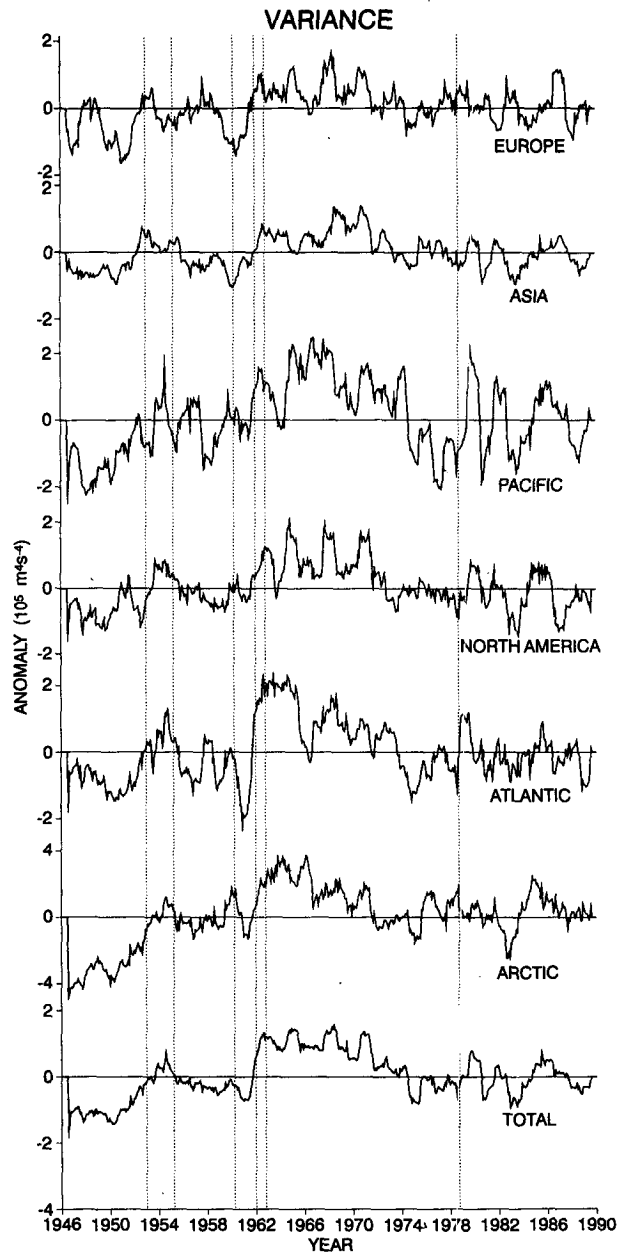


FIG. 4. Same as Fig. 3, except for the transient eddy variance of the geopotential in units of $10^5 \text{m}^4 \text{s}^{-4}$. Note the change of scale for the Arctic results.

The regional results for $\Phi'\Phi'$ are given in Fig. 4. There is only one major discontinuity present in the variance field which occurs in 1962. There is a large contribution to this jump from the Atlantic and the Arctic with lesser contributions from all other subregions. The relatively homogeneous period after 1962 indicates that the natural daily variability of the atmosphere decreased from the mid-1960s to the late 1970s and remained constant thereafter. This behavior is probably real since it is present in all the subregions.

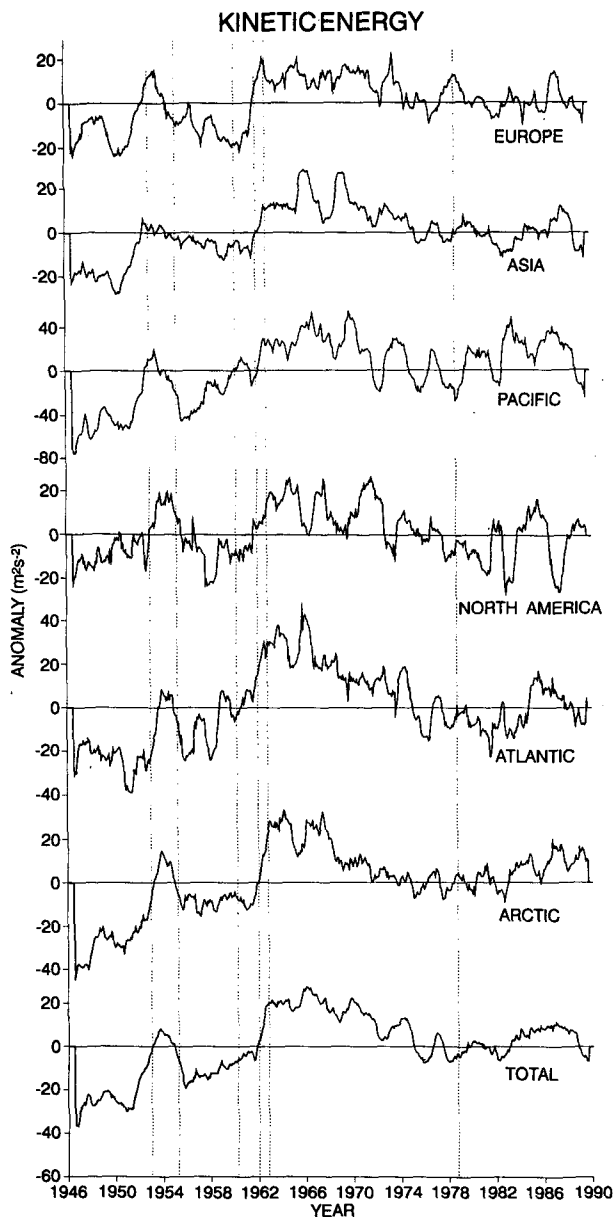


FIG. 5. Same as Fig. 3, except for the geostrophic kinetic energy. Note the change of scale for the Pacific results.

The K_g regional time series are given in Fig. 5. The interesting features of this field revealed by the unfiltered time series of Fig. 1 are the sharp discontinuity in 1962 and the increase of KE between January 1953 and March 1955. The 1962 discontinuity is evident in all the subregions. The 1953–1955 increase in K_g is evident in all regions except Asia. There is an increasing trend in the anomalies in the early 1950s which is strongest in data sparse areas. It is possible that this trend is due to improvements in the observing system rather than an increase of KE in the real atmosphere.

There are many types of studies that could make use of a long-term upper-air dataset and, consequently, the applicability of the present 500-mb dataset should be addressed. This dataset must be used with caution in those studies in which the discontinuities described could be misinterpreted as part of an expected signal. For example, there is an expected general warming of the lower troposphere and a reduction of the pole to equator temperature gradient as a result of the “greenhouse” effect. Using this 500-mb dataset one could attempt to detect the expected warming by computing 500–1000 mb thicknesses or, alternatively, one could look for a reduction of KE as a consequence of the reduced pole to equator temperature gradient. Clearly, the discontinuities in the 500-mb data could be wrongly interpreted as temperature or KE changes and as a result, caution must be exercised in applying the 500-mb data to this type of study.

In studies where the discontinuities would not be confused with an expected signal, the dataset is useful. The analyses contained in the dataset were produced mainly for weather forecasting purposes to provide the initial conditions, first for subjective, and later for machine-produced forecasts. Consequently, the dataset would likely provide a good measure of the topographical features of the 500-mb surface. Investigations, such as blocking studies or upper-level cyclone climatologies, which require such a qualitative reliability, could make use of the dataset with a relatively high degree of confidence.

5. Summary and conclusions

Long-term datasets have potential application in climate change studies. The long-term Northern Hemisphere 500-mb dataset includes analyses from many sources which have been processed using a variety of techniques. Using simple statistics the present study assesses the homogeneity of the dataset. Several discontinuities were found that coincide with known major analysis changes in 1953, 1955, 1978, and especially 1962.

If this dataset is used in climate studies then one must be aware of the analysis induced discontinuities and take them into account when interpreting the results of these studies.

Acknowledgments. The author wishes to thank Tom Chivers and Brian Taylor for drafting the figures, and Roy Jenne of NCAR who provided historical information concerning the 500-mb dataset. Finally, the assistance of the Journal Editor, R. E. Livezey, who obtained the USAF 433L ESSPO Report and suggested improvements to the manuscript, was much appreciated.

REFERENCES

- Barnston, A. G., and R. E. Livezey, 1987: Classification, seasonality, and persistence of low-frequency atmospheric circulation patterns. *Mon. Wea. Rev.*, **115**, 1083–1126.
- Berry, F. A., W. H. Haggard and P. M. Wolff, 1953: 500 millibar studies at Project AROWA. *Bull. Amer. Meteor. Soc.*, **34**, 444–453.
- Esbensen, S. K., 1984: A comparison of intermonthly and interannual teleconnections in the 700-mb geopotential height field during the Northern Hemisphere winter. *Mon. Wea. Rev.*, **112**, 2016–2032.
- Jenne, R. L., 1975: Datasets for meteorological research, NCAR-TN/IA-111, Atmospheric Technology Division, National Center for Atmospheric Research, Boulder, Colorado, 194 pp.
- Oort, A., 1983: Global atmospheric circulation statistics, 1958–1973. NOAA Professional Paper No. 14, U.S. Government Printing Office, Washington, D.C., 150 pp.
- Trenberth, K. E., and D. A. Paolino, 1980: The Northern Hemisphere sea level pressure dataset: trends, errors, and discontinuities. *Mon. Wea. Rev.*, **108**, 855–872.
- USAF Weather Observing and Forecast System, 433L, 1959: Reference manual for climatic data computer tapes. Rep. of USAF Weather Observing and Forecasting System, 433L ESSPO (JOINT), Waltham, MA, 5 pp.